

**Electronic Supplementary Information for
Reaction Mechanism and Kinetics for Ammonia Synthesis on the Fe(211) Reconstructed
Surface**

Jon Fuller¹, Alessandro Fortunelli^{2,3*}, William A. Goddard^{2*}, and Qi An^{1*}

¹Department of Chemical and Materials Engineering, University of Nevada – Reno, Nevada
89577, United States

²Materials and Procs Simulation Center (MSC), California Institute of Technology, Pasadena,
California 91125, United States

³CNR-ICCOM, Consiglio Nazionale delle Ricerche, ThC2-Lab, Pisa, 56124, Italy

Table of Contents:

Supplemental Simulation Procedures and Information

- 1. Surface Energy Details**
- 2. Fe(211) Missing Row Reconstruction Comparison**
- 3. Fe(211)R Detailed Reaction Pathway**
- 4. Fe(211)R Detailed Alternate Reaction Pathway**

Supplemental Data Items

Fig S1-12

- Fig S1 Surface energy comparison for Fe(211), Fe(111) and Fe(211) MR
- Fig S2&3 Potential energy curves for main pathway hydrogenation transition states
- Fig S4 Potential energy curves for main pathway nitrogen dissociation transition states
- Fig S5 Potential energy curves for alternate pathway nitrogen dissociation transition states
- Fig S6&7 Geometry and migration methods for hydrogenation of NH_x species on surface
- Fig S8 Alternate pathway comparison for main reaction barrier (2N-N₂ -> 4N initial)
- Fig S9 Energy level diagram at 673K, 20 atm with P(NH₃) = 1.5 torr.
- Fig S10 Spin and charge comparison for main and alternate synthesis pathways
- Fig S11 Preferred surface reconstruction comparison for Fe(211) 4H and Fe(211) MR 4H
- Fig S12 Complex N₂ Dissociation Pathway
- Fig S13 Wulff shape for bare surface and N absorbed surface at T = 0 K

Supplemental Simulation Procedures and Information

1. Surface Energy Details

Surface energies for the Fe(111), Fe(211) and Fe(211) MR surfaces were calculated according to the formula:

$$E_{\text{surface}} = E_{\text{top}} + E_{\text{bottom}} = (E_{\text{slab}} - N \cdot E_{\text{bulk/atom}}) / A \quad (1)$$

Where E_{surface} corresponds to the reported surface energy value in eV, E_{top} is the energy of the top of the slab in eV, E_{bottom} is the energy of the bottom of the slab in eV, E_{bulk} is the energy of bulk Fe atoms in eV, N is the number of atoms in the slab and A is the area of the slab in \AA^2 . For simplicity of calculations, the slab was constructed with 13 layers of Fe atoms; the top and bottom layers were allowed to relax while the central layers were fixed. This forces $E_{\text{top}} = E_{\text{bottom}}$, so $E_{\text{surface}} = 2 \cdot E_{\text{top}}$ and thus E_{surface} can be calculated as:

$$E_{\text{surface}} = ((E_{\text{slab}} - N \cdot E_{\text{bulk/atom}}) / A) / 2 \quad (2)$$

For at-temperature calculations phonon adjustments were included for both small molecules and all Fe atoms allowed to relax in the calculations.

At $T = 0\text{K}$ for blank surfaces, our numbers vary from previous theoretical research using the PBE functional; we obtain energies for the Fe(111) surface (3.233 J/m^2) and Fe(211) surface (3.300 J/m^2) that differ from previously reported results for Fe(111) (2.70 J/m^2) and Fe(211) (2.58 J/m^2);¹ although the method of calculation is similar the reasons for this discrepancy are most likely related to the selection of the slab parameters.

2. Fe(211) Missing Row Reconstruction Comparison

To determine the preferred surface configuration between the default Fe(211) surface and the Fe(211) missing row reconfiguration, both surfaces were optimized in the presence of four hydrogen atoms adsorbed in the theoretically determined position in the case of Fe(211)² and the experimentally determined position in the case of Fe(211)R¹.

Since surface reconstruction of Fe(211) has been determined experimentally in prior research to be hydrogen-induced similar to other BCC metals, the maximum amount of stable adsorbed hydrogen atoms were included for surface energy testing to ensure accurate calculations. By using the calculation method detailed in Section 1, the surface energies of Fe(211) 4H and Fe(211)R 4H were determined and can be found in Fig. S12.

From these results we calculate that Fe(211)R has a lower surface energy and conclude that the missing row reconfigured surface is more stable than the Fe(211) unreconstructed surface, making Fe(211)R the dominant surface in the presence of hydrogen. Our calculated Fe(211) surface energy at $T=673\text{K}$ (2.693 J/m^2) is in reasonable agreement with previous theoretical research using the PBE functional at 675K (2.28 J/m^2).³

3. Fe(211)R Detailed Reaction Pathway

- 3.1. 3N-NH₂-2H: We found that the 3N-NH₂-2H state, formed by surface addition of H₂ from the gas phase has a free energy of $\Delta G = -0.05$ eV.
- 3.2. 3N-NH₃-H: We found the 3N-NH₃-H configuration is formed by Langmuir-Hinshelwood migration of the newly bound H with a free energy of $\Delta G = -0.15$ eV. We found the transition state here to have a free energy of $\Delta G = 0.98$ eV. Details on this process can be found in Fig. 3.
- 3.3. 3N-H: Next, NH₃ desorbs from the surface with the desorption transition state detailed below. We found the resulting state to have a free energy of $\Delta G = 0.03$ eV with the desorption step having a free energy of $\Delta G^\ddagger = 0.98$ eV.
- 3.4. 2N-NH: The 2N-NH state likewise results from H migration across the surface as detailed in Fig. 3 and the SI, resulting in $\Delta G = -0.10$ eV and $\Delta G^\ddagger = 0.97$ eV for the H transition state.
- 3.5. 2N-NH-2H: H₂ bonds to the surface in this step similar to step 3.1 to facilitate further progress in the reaction pathway. We found a free energy of $\Delta G = -0.53$ eV for this state, the second lowest in the main reaction pathway.
- 3.6. 2N-NH₂-H: Following H migration across the surface, the 2N-NH₂-H state is produced with a free energy of $\Delta G = 0.14$ eV. We found the transition state for the H migration to have $\Delta G^\ddagger = 0.75$ eV.
- 3.7. 2N-NH₃: A second round of H migration across the surface produces the second NH₃ for the reaction pathway with a free energy calculated to be $\Delta G = 0.29$ eV with $\Delta G^\ddagger = 0.87$ eV for the transition state.
- 3.8. 2N: Desorption of the second NH₃ produces a 2N state with both remaining nitrogen atoms adsorbed to the surface located in the trough region of the second layer. We found this state to have a free energy of $\Delta G = 0.41$ eV with the NH₃ desorption having $\Delta G^\ddagger = 1.24$ eV.
- 3.9. 2N-N₂ (top): To facilitate restoration to the 4N state for a continuous pathway, a N₂ molecule binds perpendicular to the surface atop the first row Fe ridge. The NN bond distance is 1.14 Å and the N-Fe bond distance is 1.83 Å. This process is illustrated in Fig. S9. This state was found to have a free energy of $\Delta G = 0.33$ eV.
- 3.10. 2N-N₂ (bottom): The 2N-N₂ state produces migration of the adsorbed N₂ to the second-row site while remaining arranged perpendicular to the surface. The NN bond distance is 1.14 Å and the N-Fe bond distances are 1.84/2.44 Å. We found the free energy for this “bottom” site to be $\Delta G = 0.86$ eV with a transition state found to have $\Delta G^\ddagger = 1.15$ eV and an N₂ desorption with $\Delta G^\ddagger = 1.16$ eV.
- 3.11. 2N-N₂ (final): Finally, the adsorbed N₂ tilts to an almost-parallel position on the surface in preparation for dissociation of the N₂ bond to form a 4N state. The NN bond distance is 1.21 Å and the N-Fe bond distances are 1.90/2.03/2.03/2.37 Å. The free energy for this “final” site was found to be $\Delta G = 0.67$ with a transition state having $\Delta G^\ddagger = 1.04$ eV and N₂ desorption with $\Delta G^\ddagger = 1.24$ eV.

3.12a) 4N(initial): After dissociation of the N₂ bond, the initial 4N state is formed with both adsorbed second row N located adjacent to each other in 3-fold sites. The NN bond distance changes from 1.21 to 1.71 while the N-Fe bond distances change from 1.90 Å to 1.97 Å and ~2.0 Å to 1.85 Å. We found the free energy for this initial 4N state to be $\Delta G = 0.67$ eV, with the transition having $\Delta G^* = 1.55$ eV and a N₂ desorption value of $\Delta G^\circ = 1.31$ eV. This transition state represents the primary barrier for the main pathway.

3.12b) 4N*: The 4N initial state then transitions to the 4N* state by migration of one N across the ridge to the second layer site on the opposite side via diffusion mechanism with a 0.32 eV barrier. The free energy for this 4N* state was calculated to be $\Delta G = -0.75$ eV. We found the transition state for this process to be $\Delta G^* = 0.98$ eV.

3.12c) 4N**: The 4N* state will transform to an even lower structure 4N** by migration of two N atoms from the top layer to the 2nd second layer (Fig. 4) via diffusion mechanism with a 0.25 eV barrier. The free energy for this 4N** state was calculated to be $\Delta G = -0.98$ eV. We found the transition state for this process to be $\Delta G^* = -0.50$ eV. The 2nd layer N is strongly bonded to Fe(211)R surface and we assume it transform to 4N* state for following hydrogenation. The barrier from 4N** to 4N* is computed to be 0.48 eV.

3.13. 4N-2H: H adsorbs to the surface as in previous steps to facilitate continuation of the synthesis reaction. We calculated the free energy for this step to be minimal (~0.01 eV) and thus is omitted here.

3.14. 3N-NH-H: NH is formed on the surface via Langmuir migration to form the 3N-NH-H state. We calculated $\Delta G = -1.04$ eV for this step, with Eley-Rideal (ER) hydrogenation of $\Delta G^* = 0.60$ eV.

3.15. 3N-NH₂: The second H adsorbed to the surface then migrates to form the 3N-NH₂ state with $\Delta G = -0.54$ eV. This state is used for $\Delta G = 0$ eV as previously.⁷ This complete the synthesis reaction pathway.

Transition states and desorption steps with a significant effect on the reaction barrier are listed below in further detail, in order from highest barrier to lowest at T = 673 K, P(NH₃) = 1 atm for the reaction pathway. Detailed information for main pathway transition states, including energy curves can be found in Fig. S2-S6 of SI.

- TS12a – The primary barrier for the reaction is represented here by the dissociation of the adsorbed N₂ to form the initial 4N state. At this transition state, the adsorbed N₂ begins the dissociation process with the bond lengthening from 1.21 Å to 1.71 Å, indicating that the bond has been reduced to an elongated single bond before separation.
- 7-NH₃ desorption – The highest barrier for the reaction pathway found outside of the steps restoring to the 4N state is the desorption of the second NH₃ molecule with $\Delta G^\circ = 1.24$ eV.
- 9-N₂ desorption – The second-highest barrier for the reaction is found in the N₂ desorption step for N₂ migration to the deep state on the second Fe layer. The N₂

molecule remains adsorbed in a slightly tilted perpendicular position with $\Delta G^\circ=1.16$ eV and a NN bond length of 1.14 Å.

- 8-N₂ adsorption– Adsorption of the N₂ molecule for the 2N-N₂ state was found to have a ΔG° value of 1.15 eV. The N₂ molecule adsorbs in a perpendicular position on the first Fe layer with NN bond length of 1.14 Å.
- 7-NH₃ desorption – The highest barrier for the reaction pathway found outside of the steps restoring to the 4N state is the desorption of the second NH₃ molecule with $\Delta G^\circ=1.24$ eV.
- TS10 – The migration of the adsorbed N₂ molecule from the top to bottom positions (in the perpendicular configuration described above) was found to have a free energy difference of $\Delta G^*=1.15$ eV.

4. Fe(211)R Alternate Pathway

In order to find a lower reaction barrier, we evaluated the alternative pathway with the presence of additional 2H on the surface for high-barrier steps including the 2N-N₂ migration and dissociation pathway along with the second NH₃ desorption step. We used a similar approach for the (111) studies with significant results.⁹ We found that the addition of the 2H atoms significantly lowered the barrier for all key states in the N₂ dissociation pathway. The states found in this pathway along with their ΔG values relative to the 3N-NH₂ reference state are detailed below. Detailed information on alternate pathway transition states, including energy curves, are found in Fig. S7-S8 of SI.

4.7. 2N-2H-NH₃: In the alternate pathway, 2H adsorbs to the surface in the bottom positions opposite the active sites for NH₃ desorption and later N₂ adsorption. $\Delta G = -0.02$ was found for this position relative to the reference state.

4.8. 2N-2H: Similar to the main pathway, NH₃ desorbs from the top site leaving the 2N-2H state. We found the free energy for this state to be $\Delta G = -0.22$, with the NH₃ desorption of $\Delta G^\circ = 0.77$. This is significantly lower than the main pathway NH₃ desorption value.

4.9. 2N-2H-N₂ (top): N₂ again binds to the surface in a perpendicular configuration atop the ridge opposite the adsorbed H species with $\Delta G = -0.14$.

4.10. 2N-2H-N₂ (bottom): The adsorbed N₂ species migrates to the bottom position with $\Delta G = 0.25$ and a transition state with $\Delta G^* = 0.70$. We found N₂ desorption to have $\Delta G^\circ = 0.76$.

4.11. 2N-2H-N₂ (final): As in the main pathway the adsorbed N₂ tilts and rises off the surface to assume a final position prior to dissociation with $\Delta G = 0.35$ and $\Delta G^* = 0.55$ for the transition state. We found the N₂ desorption to have $\Delta G^\circ = 0.71$ for this step.

4.12a) 4N-2H (initial): The post-dissociation state was found to have $\Delta G = 0.15$, with a transition state with free energy of $\Delta G^* = 1.14$ and N₂ desorption energy of $\Delta G^\circ = 0.84$.

The new barriers for the high-barrier steps in this alternate 2H-added pathway, again at T = 673 K and P NH₃ = 1 atm, are listed below in order of decreasing ΔG values:

- TS12a (2H) – Addition of two H atoms adsorbed to the surface opposite the N₂ significantly lowers the barrier presented by this transition state from $\Delta G = 1.55$ eV to $\Delta G^* = 1.14$ eV. This transition state remains the overall energy barrier for the reaction.
- 12-N₂ desorption – Likewise, the presence of 2H adsorbed to the surface lowers the barrier here to $\Delta G^{\ddagger} = 0.84$ eV.
- 9-N₂ adsorption – We found the initial N₂ molecule adsorption on the top position to have a much lower free energy of $\Delta G^{\ddagger} = 0.76$ eV in the alternate pathway.
- 8-NH₃ desorption – Previously representing the highest barrier outside of the 4N restoration process, we found the second NH₃ molecule desorption step to have a free energy of $\Delta G^{\ddagger} = 0.77$ eV in the alternate pathway.
- TS11 – We found a significantly lower free energy difference of $\Delta G^* = 0.70$ eV for the transition state here in the alternate pathway.

Supplemental Data Items

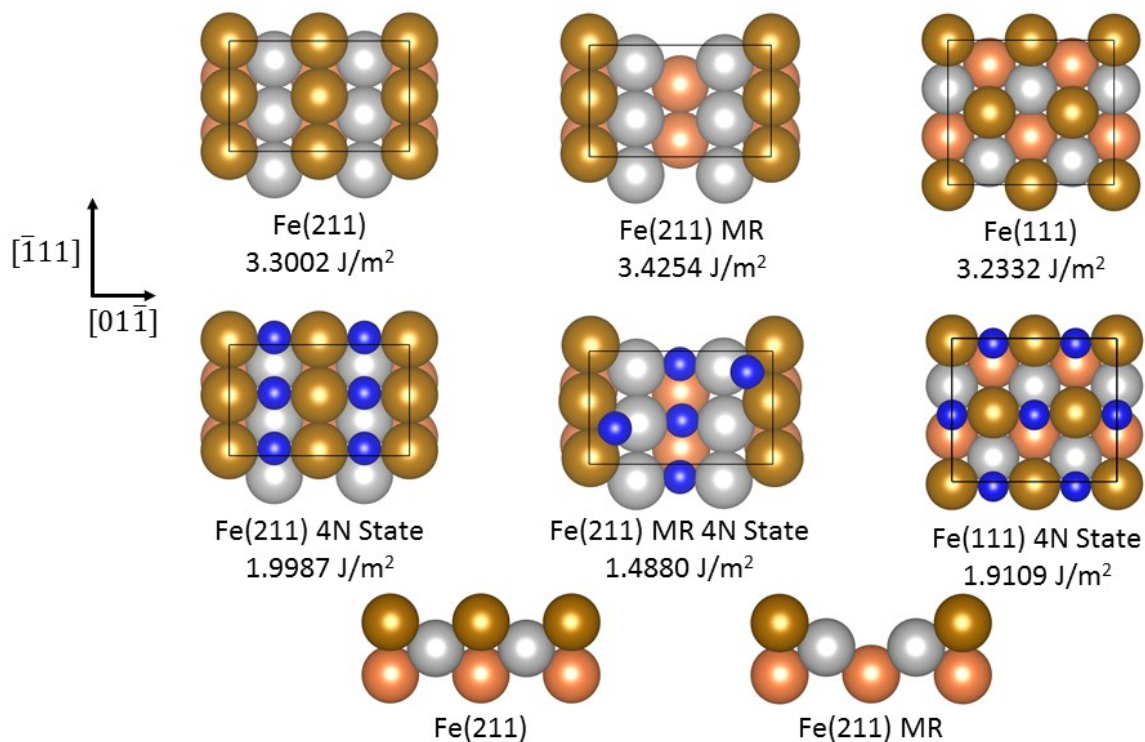


Fig. S1 - Surface comparison of the Fe(211), Fe(211) with missing row reconstruction, and Fe(111) surfaces using PBE-D3 functional at $T = 0$ K, related to Fig. 3. First layer atoms are denoted by bronze spheres, second layer atoms are denoted by silver spheres, and third layer atoms are denoted by peach spheres. Only the top three layers (out of six) are shown here. Note the missing central row of first layer Fe atoms in the missing row configuration. 4N states are also presented for comparison, with blue spheres denoting nitrogen atoms.

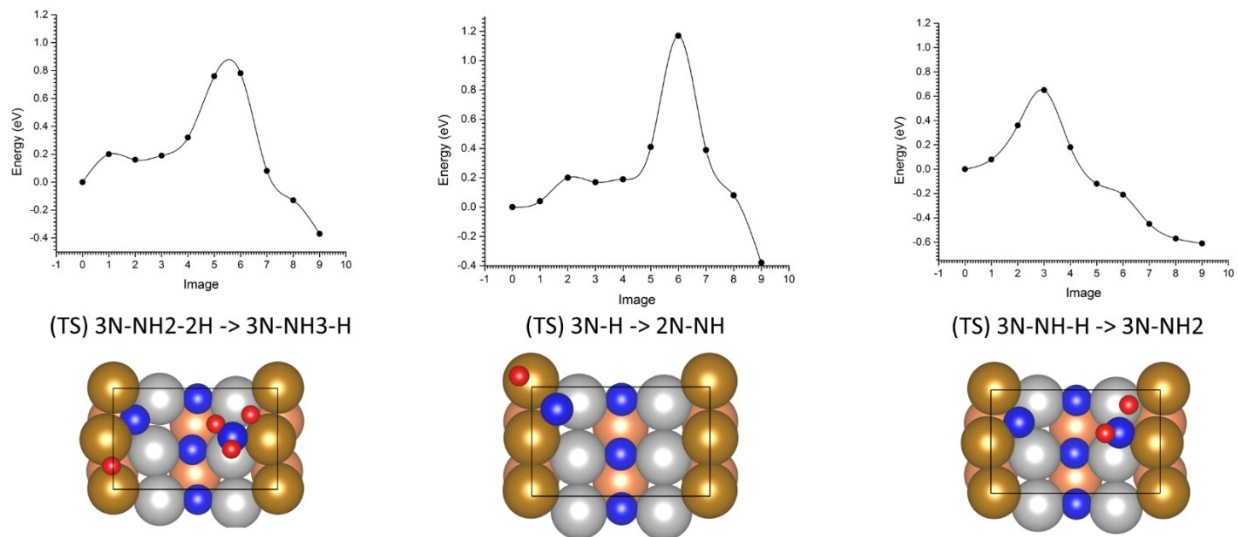
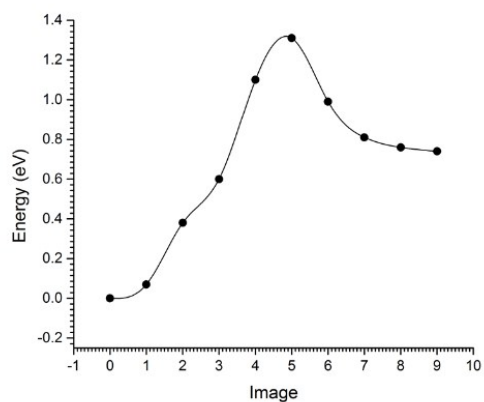
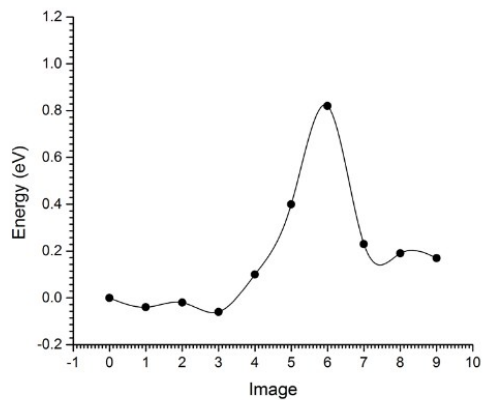
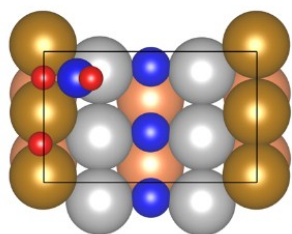


Fig. S2 – Climbing Nudged Elastic Band (NEB) results for main pathway hydrogenation transition states are shown above in terms of energy in eV, related to Fig. 3. The NEB method generates a true transition state verified by phonon calculations identifying a single negative curvature in the Hessian. Dimer calculations were performed for all negative frequencies calculated from the NEB images.



(TS) 2N-NH-2H -> 2N-NH2-H



(TS) 2N-NH2-H -> 2N-NH3

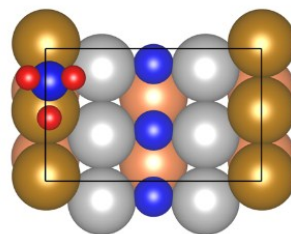


Fig. S3 – Climbing Nudged Elastic Band (NEB) results for main pathway hydrogenation transition states are shown above in terms of energy in eV, related to Fig. 3. The NEB method generates a true transition state verified by phonon calculations identifying a single negative curvature in the Hessian. Dimer calculations were performed for all negative frequencies calculated from the NEB images.

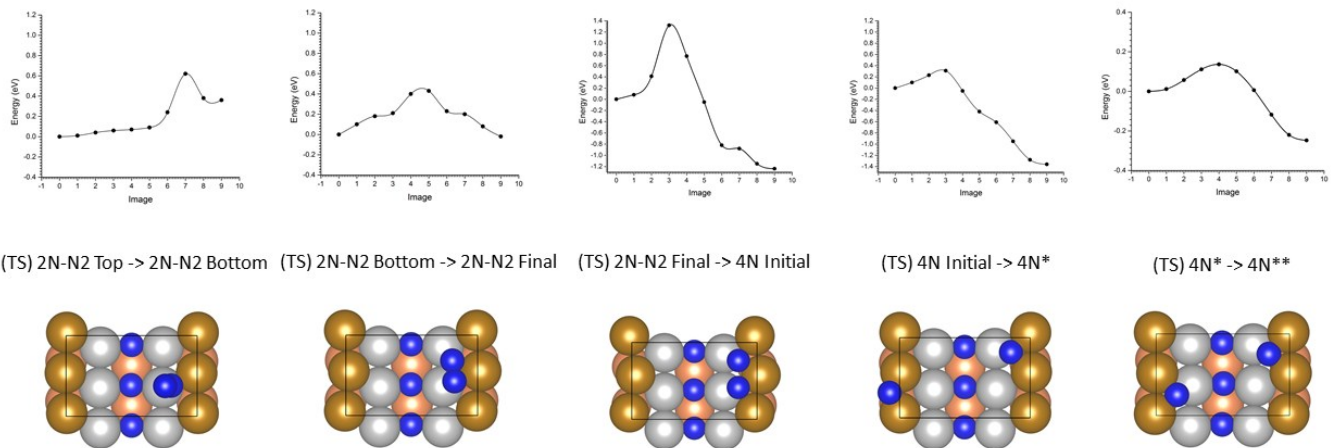


Fig. S4 – NEB results for main pathway N2 dissociation transition states are shown above in terms of energy in eV, related to Fig. 4. The NEB method generates a true transition state verified by phonon calculations identifying a single negative curvature in the Hessian. Dimer calculations were performed for all negative frequencies calculated from the NEB images.

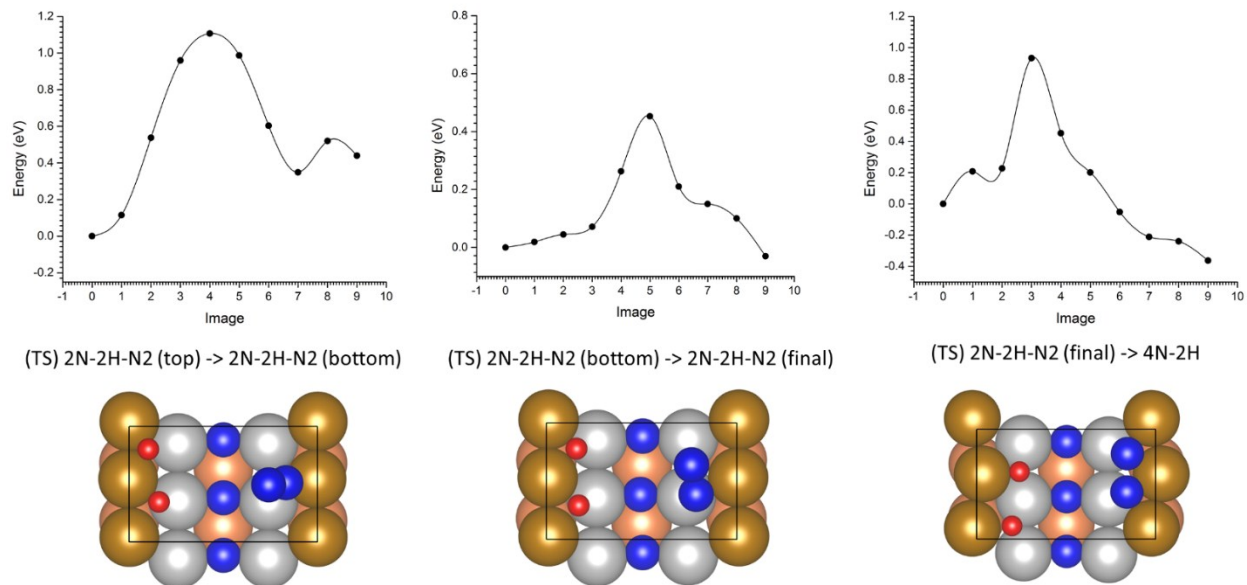


Fig. S5 – NEB results for alternate pathway N2 dissociation transition states are shown above in terms of energy in eV, related to Fig. 4. The NEB method generates a true transition state verified by phonon calculations identifying a single negative curvature in the Hessian. Dimer calculations were performed for all negative frequencies calculated from the NEB images.

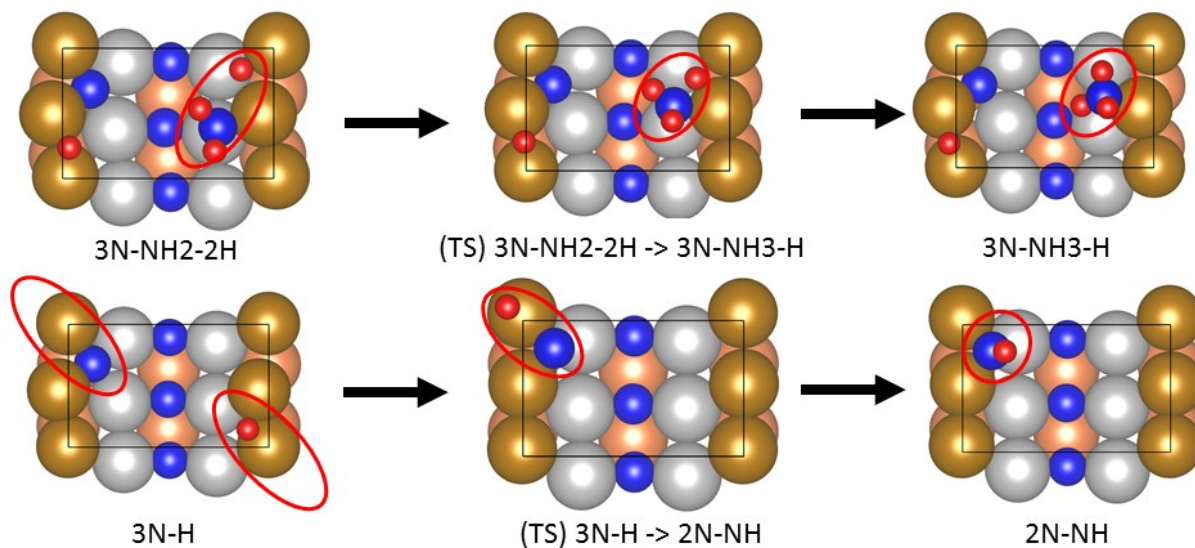


Fig. S6 – Methods of H migration to form NH_3 and NH are shown. Hydrogen bonds to the N/NH species via Langmuir-Hinshelwood mechanism to form the new NH_x species, related to Fig. 3. Key reaction species are circled in red for each state.

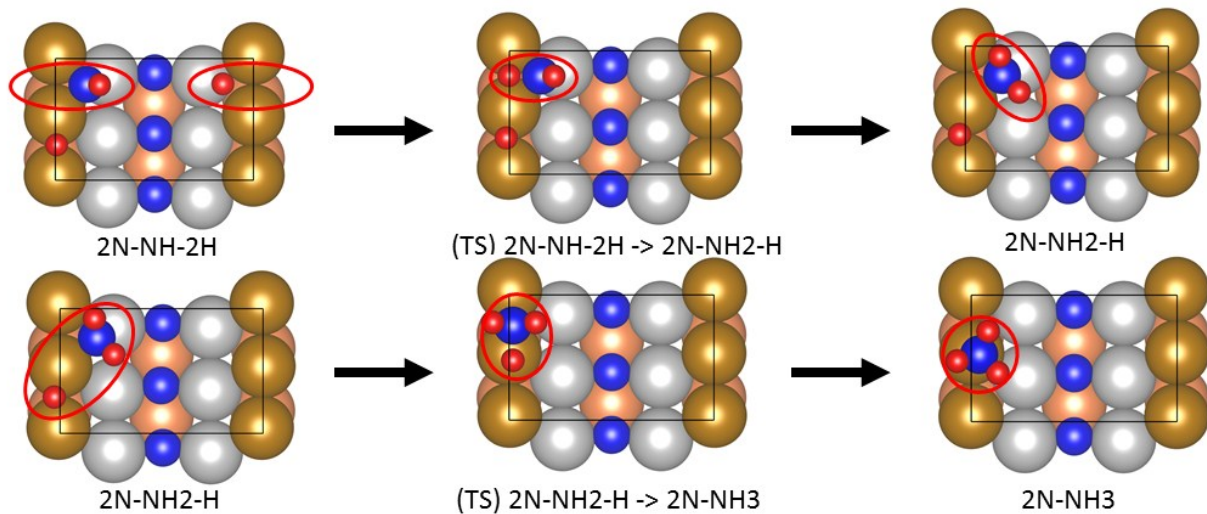


Fig. S7 – Methods of H migration to form NH_2 and second NH_3 are shown. As above, the Langmuir-Hinshelwood mechanism is employed for production of NH_x species, related to Fig. 3. Key reaction species are circled in red for each state.

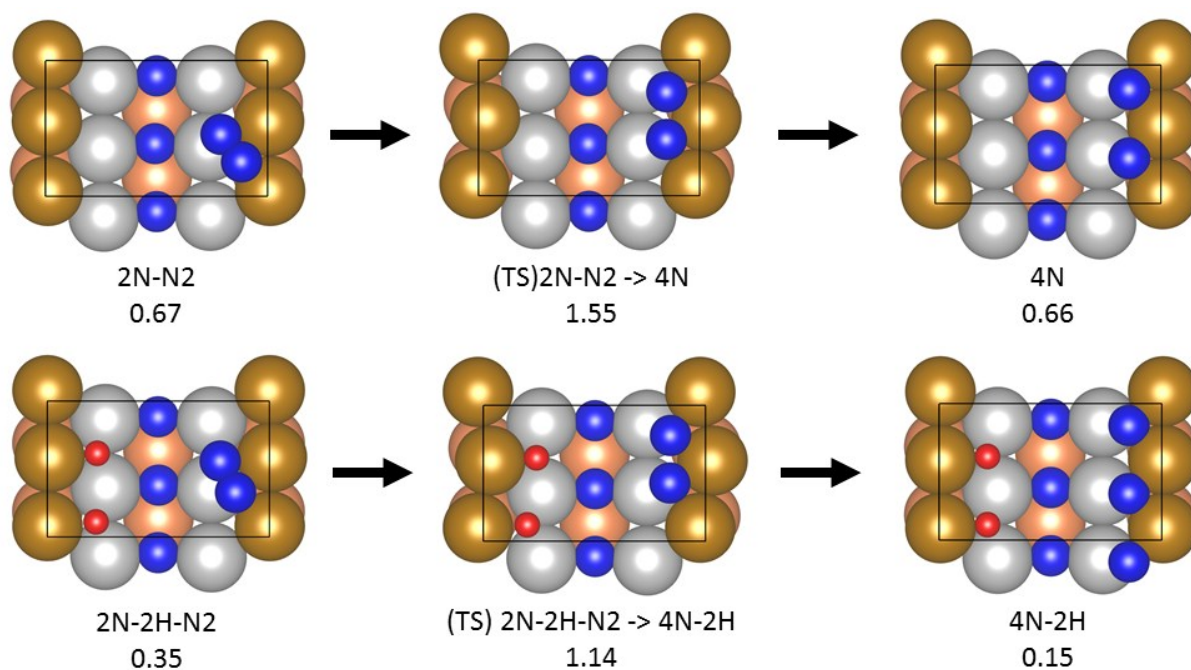


Fig. S8– Alternative pathway tested for reduction of overall barrier is shown here, related to Fig. 3 and Fig. 4. The 2N-2H-N₂ -> 4N-2H pathway was found to be most effective for reduction of the primary reaction barrier, reducing the dissociation ΔG^* from 1.55 eV to 1.14 eV. ΔG and ΔG^* are presented below each state in eV.

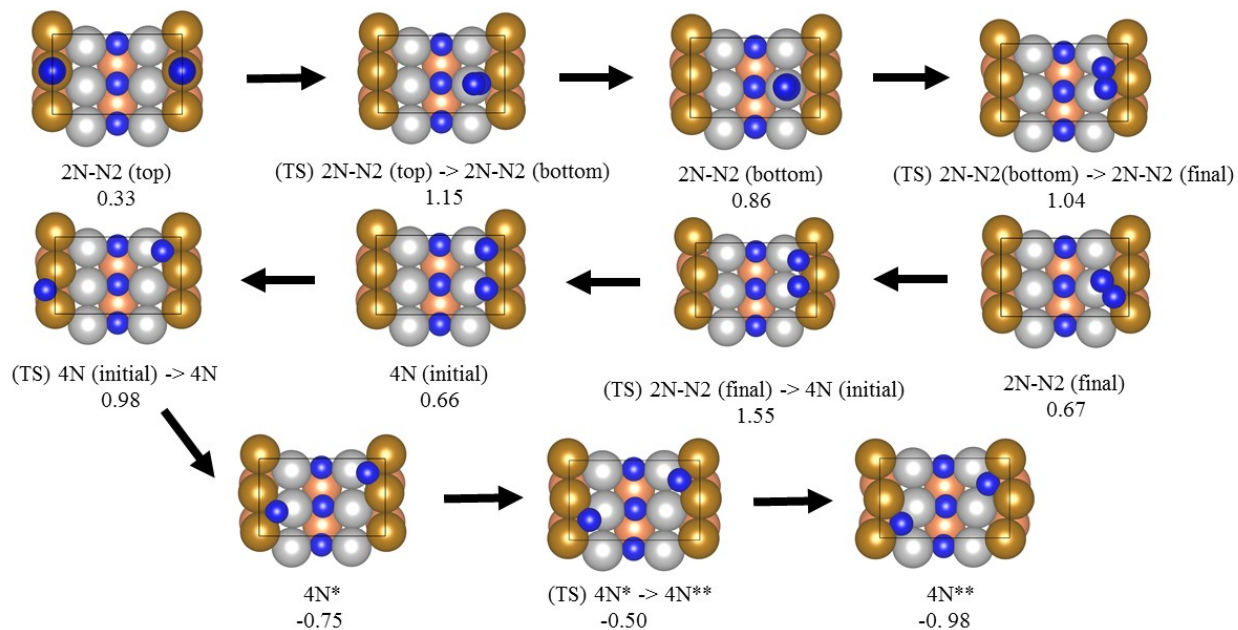


Fig. S9 – The $2N-N_2 \rightarrow 4N$ pathway shown in greater detail. For the perpendicular N_2 molecule the lower N atom is enlarged slightly for clarity. Slight tilting away from the first-row Fe atoms is observed in both the transition to and in the bottom position. The N_2 bond lengthens beginning with the transition between the bottom and final states, eventually separating to form the 4N (initial) state. N then diffuses across ridge to form the $4N^*$ state. $4N^*$ transitions to $4N^{**}$ in which the N atoms are very strongly bound to the surface.

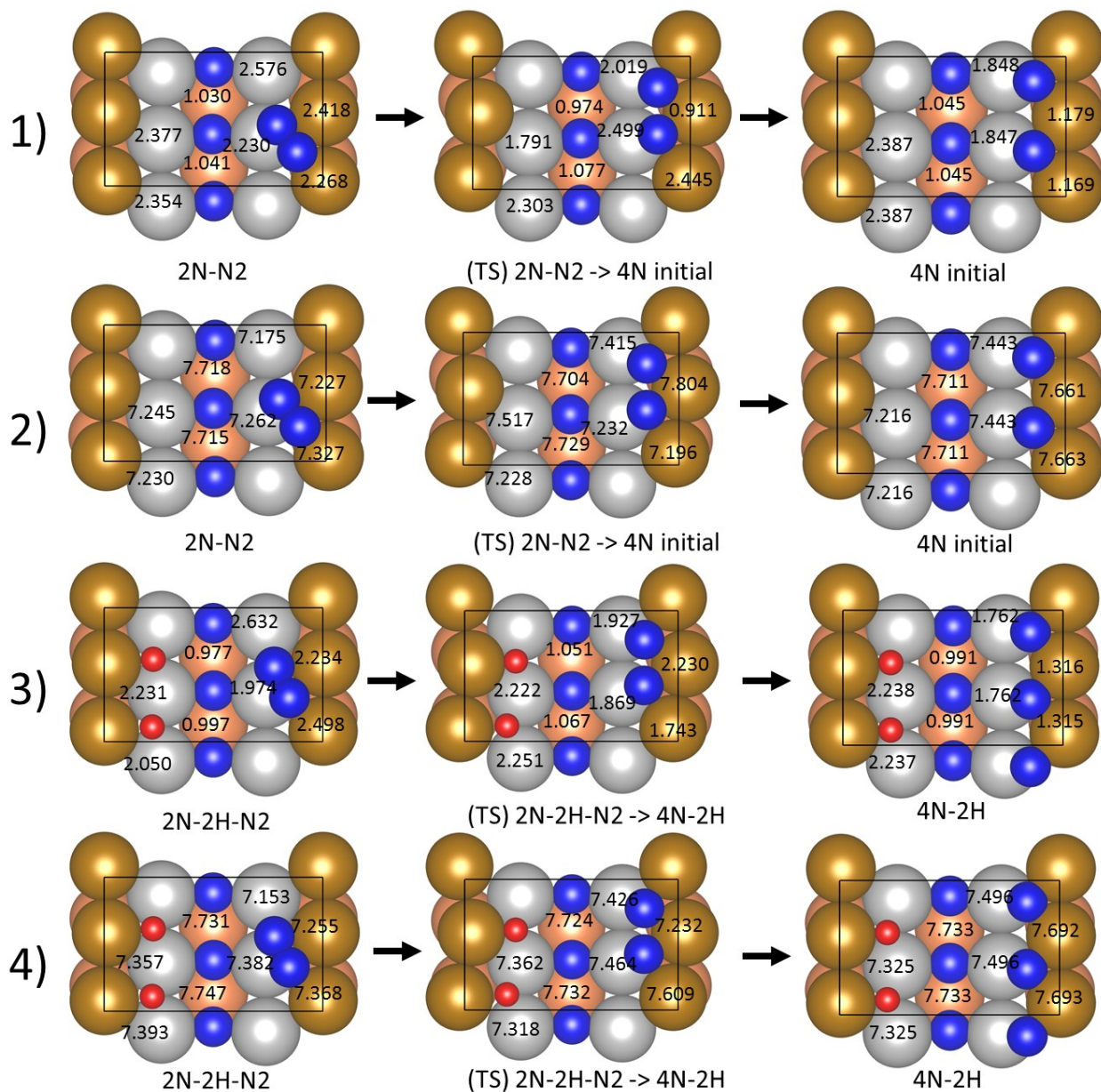


Fig. S10 - Spin and charge changes during N₂ dissociation on surface Fe (first, second and third layers) are presented the main dissociation pathway, related to Fig. 3 and Fig. 4. 1) and 3) show the spin changes in Fe atoms during dissociation for the main and alternate pathways, while 2) and 4) illustrates the charge differences in Fe atoms during dissociation for those states.

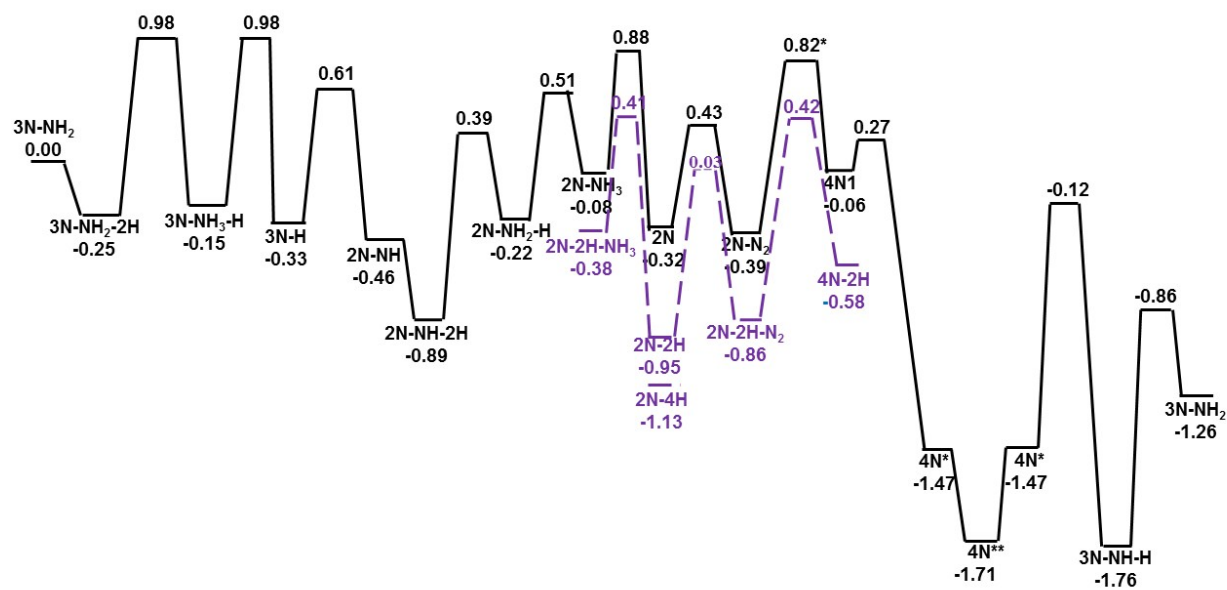


Fig. S11– Fe(211) MR NH_3 synthesis free energy diagram at 673K, $P(\text{H}_2) = 15$ atm, $P(\text{N}_2) = 5$ atm, and $P(\text{NH}_3) = 1.5$ torr, related to Fig. 2. ΔG is represented in eV; 3N-NH_2 is used as the reference state. Alternate pathway including 2H is shown in purple.

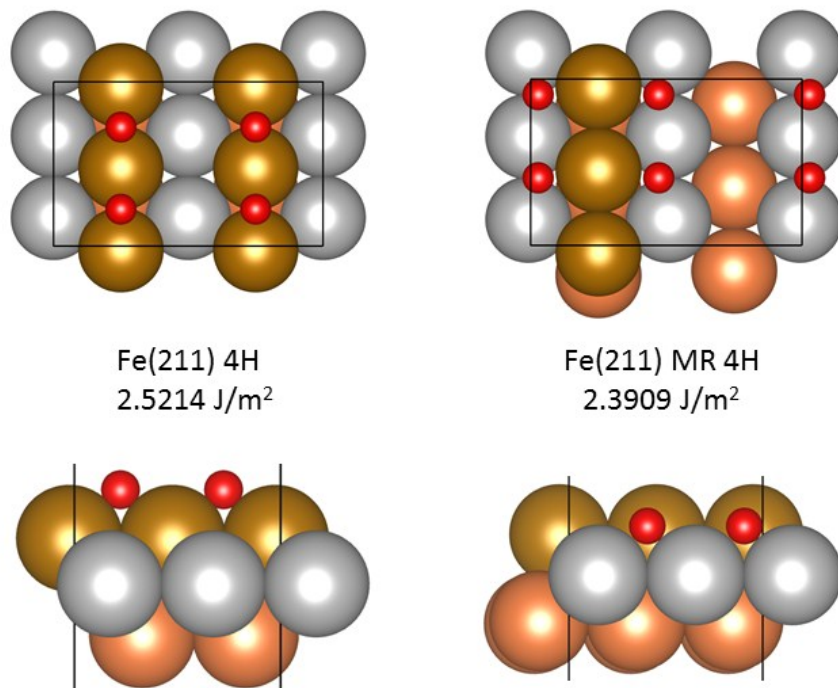


Fig. S12 – Fe(211) and Fe(211)R 4H states energy comparison in J/m², related to Fig. 1. Surface energies calculated according to method described in Section 1 of SI; Fe(211)R found to be more stable (and thus preferential) surface in presence of hydrogen adsorbed to surface.

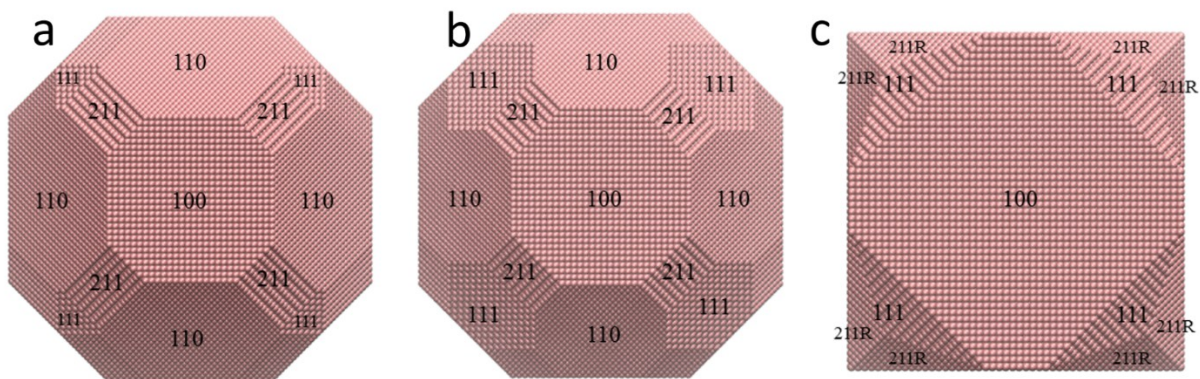


Fig. S13 – Equilibrium Wulff shape for bare surface and N-adsorbed surface at $T = 0$ K. From left to right: (a) depicts the calculated Wulff shape using surface energy values for various surface orientations obtained by Tran et. al⁴ (PBE functional) while (b) depicts the calculated Wulff shape using surface energy values calculated using the PBE-D3 functional in our research. The surface energy we calculate for Fe(211) in (b) is similar to Fe(111) and thus the facet size is increased, while the Fe(211) surface energy is lower than Fe(111) in Tran’s work so the facet size is smaller in (a).⁴ Unreconstructed Fe(211) energy is used in both (a) and (b) as it is found to be lower than Fe(211)R for the bare surface. (c) depicts the equilibrium Wulff shape for the $P(N_2)=5\text{atm}$ nitrogen-adsorbed system. Fe(211R) is found to have notably lower surface energy than Fe(211) and Fe(111) in this configuration while Fe(110) is significantly higher, leading to a change in shape configuration.

Table S1 – Comparative Data on preferred sites, bond length and adsorption energy of species involved in the NH₃ synthesis reaction on Fe(211) surface, related to Fig. 1. 211 MR calculations performed with PBE-D3 functional and 211 calculations taken from McKay et. al using PW91 functional. Similar positions and bond length are found for all cases accounting for difference in surface construction, with differences in binding energy as predicted in their work.²

Species	Preferred Sites (211 MR)	Preferred Sites (211) ⁸	Primary Bond Length (211 MR) in Å	Primary Bond Length (211) in Å ⁸	Adsorption Energy (211 MR) in eV	Adsorption Energy (211) in eV ⁸
H	Top, Bridge	Top, Bridge	1.77	1.69	0.62	0.70
N	Bottom	Bottom	1.83	1.82	1.52	1.72
N ₂	Top, Bottom, Climbing	Bottom	1.80	1.89	1.17	1.84
NH	Bottom	Bottom	2.02	1.97	1.35	2.04
NH ₂	Climbing	Bridge	2.06	1.94	1.24	2.00
NH ₃	Top	Top	2.10	2.09	0.49	0.79

Table S2. HB catalytic reaction rates under steady-state conditions on (2x2) unit cells of the Fe(111) and reconstructed Fe(211) surfaces as predicted by DFT/kMC simulations, related to Fig. 5. Rates in molecules of NH₃ produced per (2x2) unit cell per second. Pressures in atm.

P(H ₂)	P(N ₂)	P(NH ₃)	Fe(111)	Fe(211)
5	5	1.5/760	21.7	8.2
5	5	1	1.2	0.15
15	5	1.5/760	26.8	18.7
15	5	1	4.6	3.45
22	5	1.5/760	23.0	20.7
22	5	1	5.1	5.7
30	5	1.5/760	19.2	20.2
30	5	1	5.1	8.0
40	5	1.5/760	15.6	18.0
40	5	1	4.9	9.7
50	5	1	-	9.8
60	5	1	-	9.6
150	50	1	24.6	32.6
120	40	20	2.3	10.0
200	50	1	-	26.8
170	40	20	-	11.8
250	50	1	18.2	22.6
220	40	20	2.1	12.2
300	50	1	-	19.3
270	40	20	-	12.3

Table S3. Calculated surface energy values for Fe(100), Fe(110), Fe(111), Fe(211), and Fe(211)R at T = 0 K and 673 K for bare surface, and T = 0 K and 673 K, and P(N₂)=5 atm for nitrogen-adsorbed surfaces using PBE-D3 functional. Comparative surface energy values found by Tran et. al are included as well.⁴ Note that Fe(211)R values are not provided in Tran et. al's work.

Surface Orientation	Bare surface at T=0K (PBE-D3; unit: J/m ²)	Bare surface at T=673K (PBE-D3; unit: J/m ²)	Bare surface (PBE; unit: J/m ²) ⁴	Nitrogen-adsorbed surface at T=0K and P(N ₂)=5atm (PBE-D3 unit:J/m ²)	Nitrogen-adsorbed surface at T=673K and P(N ₂)=5atm (PBE-D3 unit: J/m ²)
100	3.148	2.369	2.50	1.221	1.069
110	3.138	2.158	2.45	2.045	-
111	3.233	2.856	2.73	1.911	2.127
211	3.300	2.693	2.61	1.999	2.418
211R	3.425	2.897	-	1.488	1.924

Supplementary References

- (1) T. Wang, X. Tian, Y. Yang, Y-W. Li, J. Wang, M. Beller, and H. Jiao, Coverage-Dependent N₂ Adsorption and Its Modification of Iron Surfaces Structures, *J. Phys. Chem. C.*, 2016, **120**, 2846-2854
- (2) H. McKay, S. Jenkins, and D. Wales, Theory of NH_x ± H Reactions on Fe{211}, *J. Phys. Chem. C.*, 2009, **113**, 15274-15287
- (3) T. Wang, S. Wang, Q. Luo, Y-W. Li, J. Wang, M. Beller, and H. Jiao, Hydrogen Adsorption Structures and Energetics on Iron Surfaces at High Coverage, *J. Phys. Chem. C.*, 2014, **118**, 4181-4188
- (4) Tran, R., Xu, Z., Radhakrishnan, B., Winston, D., Sun, W., Persson, K., and Ong, S. P. Surface energies of elemental crystals, *Sci. Data*, 2016, **3**:160080.